Tailorable biofunctionalization of poly(acrylamide) hydrogels via firefly luciferin-bioinspired click ligation accelerates cell attachment, spreading and proliferation

*Alexis Wolfel, Minye Jin, Nuno Araújo-Gomes, Malin Becker, Jeroen Leijten, Liliana Moreira Teixeira, Julieta I. Paez**

Dr. Alexis Wolfel, Minye Jin, Dr. Nuno Aráujo-Gomes, Malin Becker, Prof. Jeroen Leijten, Dr. Julieta I. Paez
Developmental Bioengineering, TechMed Centre, University of Twente. Drienerlolaan 5, 7522NB, Enschede, The Netherlands.
E-mail: j.i.paez@utwente.nl

Dr. Liliana Moreira Teixeira
Advanced Organ Bioengineering and Therapeutics, TechMed Centre, University of Twente. Drienerlolaan 5, 7522NB, Enschede, The Netherlands.

Keywords: biofunctionalization, poly(acrylamide), hydrogels, luciferin click ligation, bioconjugation, chemical selectivity, ligand loading.

Abstract. Polyacrylamide (PAM) hydrogels are extensively used as extracellular matrix mimics to study specific cell-materials interactions. However, chemistries typically applied for biofunctionalization of PAM lack chemo-selectivity and control over ligand density, which undermine reproducibility of cellular behavior, which can lead to inconclusive experiments. In this work, we introduce firefly luciferin-inspired click ligation to enable controlled and tunable biofunctionalization of PAM hydrogels. A novel acrylamide-based co-monomer is synthesized and incorporated in PAM hydrogels using traditional protocols, which introduces cyanobenzothiazole (CBT) functional groups. CBT mediates biofunctionalization of PAM with N-Cys bearing biomolecules via luciferin click chemistry. Biofunctionalization takes place under mild conditions, with high efficiency within only a few minutes, and does not require light exposure. When compared to the current commercial gold standard for PAM biofunctionalization sulfo-SANPAH, hydrogels modified via luciferin click ligation show increased control in loading of cell-adhesive biochemical cues. This leads to increased cellular attachment, spreading and proliferation due to a more efficient, homogeneous, and functional biofunctionalization. Luciferin-inspired click ligation may become a new standard for reliable biofunctionalization of PAM hydrogels with increased control over the density and preserved function of the presented biological cues, thus allowing more robust platforms for 2D cell-materials interaction experimentation.

1. Introduction

Hydrogels are 3D crosslinked polymeric networks that can uptake large amounts of aqueous solutions. Their high water content and softness resemble that of the extracellular matrix (ECM) that supports living cells in their native microenvironment. Furthermore, the biophysical and biochemical properties of hydrogels can be tailored to design tissue-mimicking models with extensive applications in cell biology, tissue engineering, and regenerative medicine.[1] One of such synthetic hydrogels is poly(acrylamide) (PAM), which is widely used as substrate for 2D cell culture. These *in vitro* models are commonly used to investigate how cells sense and respond to variations in their microenvironment. For example, these soft substrates allow to analyze specific cell-materials interactions and effect of the matrix mechanical properties on cell adhesion, proliferation, migration, differentiation, and gene/protein expression.[2-5] PAM hydrogels offer important benefits that justify their broad use as culture platforms in cell biology laboratories: they are cost-effective and easy to synthesize, their mechanical properties can be easily customized within the physiological range of native soft tissues (e.g., elasticity in the range E= 0.1-100 kPa), their optical transparency makes them compatible with microscopy methods, and their anti-fouling properties avoid undesired unspecific interactions with biomolecules present in cell culture media.[6, 7]

Despite the mentioned advantages, precise control over PAM hydrogels biofunctionalization to introduce particular biochemical cues to study specific cell-materials interaction remains challenging. The chemical inertness of the amide side groups of PAM hampers controlled and tunable chemical conjugation of bioligands, especially under mild conditions, which are needed to preserve biofunctionality. Several chemical strategies have been developed to overcome this issue,[8] however, current approaches still fail at controlling bioligand density while preserving biofunctionality and hydrogel properties, or are too labor intensive to implement. For instance, the most broadly applied PAM biofunctionalization strategy is based on the use of

sulfosuccinimidyl 6-(4'-azido-2'-nitrophenylamino)hexanoate (known as sulfo-SANPAH, SS) as photoreactive primer onto PAM. Although SS offers the possibility to mediate bioconjugation of a variety of amine-bearing bioligands, it has several limitations that affect the reliability of the results. Previous studies reported that SS has a short half-life in solution that can affect reproducibility between replicates[9] and it has limited solubility and reactivity thus leading to insufficient conjugation efficiency.[10] Furthermore, the unspecific chemistry of SS can impair the biological function of immobilized biomolecules, overall resulting in limited control over bioligand activity upon loading to PAM.[11] Other strategies are based on the incorporation of a reactive co-monomer (e.g., acrylic acid) to which the ligand can be bound, which can offer better reproducibility and control over bioligand density, but often have undesired large impact on hydrogel properties such as noticeable increase in hydrogel swelling or opaqueness. Methylsulfonyl co-monomers were reported to improve the biological performance of PAM hydrogels by offering a chemo-selective and efficient bioconjugation strategy that preserved the biological function of ligands. On the downside, the synthesis of these co-monomers demands intense synthetic labor, which might complicate the scalability, cost-effectivity, and adoption of this strategy for general use.[11, 12] To promote more reliable and conclusive results over cell-materials interaction experiments carried out on biofunctionalized PAM substrates, more efficient and user-friendly strategies for biofunctionalization are needed.

Luciferin click ligation is a bioinspired coupling reaction that occurs in the biochemical cycle of luciferin synthesis inside of the firefly body.[13] This reaction binds covalently cyanobenzothiazole groups (CBT) and N-Cys-bearing biomolecules under mild conditions (in buffer, at neutral pH and at room temperature) with high conversion, and is light-free. This reaction has been used for bioconjugation[14] and biomedical applications due to its high efficiency under close-to-physiological conditions that makes it suitable, for example, for the

labelling of biomolecules inside of living cells[15] or *in vivo*.[16, 17] Importantly, cost-effective CBT precursors are commercially available and can be incorporated to polymeric macromers in a couple of straightforward reaction steps using inexpensive reagents. Following this approach, we recently reported the use of this click reaction to mediate hydrogel crosslinking and exploited this approach for the fabrication of cell encapsulating 3D hydrogels.[18] We envisioned that this bioconjugation strategy could be extended to the preparation of acrylic-based hydrogels for 2D cell culture, such as PAM, by incorporating pendant CBT moieties for subsequent chemo-selective bioconjugation. We hypothesized that this would facilitate a high level of control over ligand loading to PAM.

In this work, we introduce luciferin click ligation as a strategy for controlled and tunable biofunctionalization of PAM hydrogels. We synthesize an acrylamide-based co-monomer bearing CBT groups that can be easily incorporated in PAM hydrogels by common protocols of free-radical polymerization. When co-polymerized with acrylamide (AM), this new co-monomer introduces CBT groups into PAM, which enables biofunctionalization with N-Cys bearing biomolecules via luciferin click ligation. Biofunctionalization takes place by simple incubation of the derived hydrogel with a bioligand solution under mild conditions (aqueous buffer, no light exposure required) with high efficiency in a few minutes. Moreover, ligand loading can be finely controlled by adjusting reaction parameters, such as ligand concentration and reaction time. We compare our novel approach to the gold standard SS-mediated PAM biofunctionalization strategy for the culture of cells and demonstrate that PAM-CBT hydrogels outperform SS-mediated PAM system in promoting higher and faster cell attachment, spreading and proliferation. This is attributed to a more efficient and homogeneous ligand loading with preserved functionality attained in PAM-CBT substrates. Luciferin click ligation might become a new standard for the reliable biofunctionalization of PAM hydrogels with increased control over the biological properties of the substrates, especially when more responsive, homogenous,

and cytocompatible cell-culture substrates are required. These findings contribute to achieving more robust platforms for cell-materials interaction experimentation.

2. Results and Discussion

2.1. Synthesis and characterization of CBT-AM co-monomer and PAM-CBT hydrogels

To implement luciferin click ligation as a biofunctionalization strategy for PAM hydrogels, we first designed a synthetic pathway to incorporate cyanobenzothiazole (CBT) moieties into PAM gels. We envisaged that an acrylamide-based co-monomer bearing a CBT group (CBT-AM) could be co-polymerized with AM via free-radical polymerization during PAM hydrogel synthesis. A common issue with newly developed co-monomers is that their side functional group may inhibit the free-radical polymerization or may be chemically altered by the reaction.[19] Preliminary experiments carried out using a CBT precursor suggested that the CBT side group could withstand the conditions used for free-radical initiation, since the CBT integrity was preserved after being exposed to initiation conditions (as proven by ^{1}H and ^{13}C NMR spectra, see Figure S1 in the Supporting Information). These results encouraged us to use CBT-AM as co-monomer in PAM preparation.

The novel co-monomer CBT-AM was synthesized in three simple steps (**Figure 1A**). First, 2-(Boc-amino)ethyl bromide was anchored to the hydroxyl group of 2-cyano-6-hydroxybenzothiazole (CBT-OH) to act as a short spacer between CBT and the polymerizable acrylamide moiety. After removing the Boc protecting group under acidic conditions and reacting the free amine group with acryloyl chloride, the co-monomer CBT-AM was obtained. The purified co-monomer was characterized by NMR, UV/Vis, IR spectroscopy, mass spectrometry, and analytic HPLC. Details are presented in Figure S2. In relation to previously reported methylsulfonyl co-monomers,[11] the synthesis of CBT-AM is shorter (i.e., 3 synthetic steps for CBT-AM vs the 4-5 steps required for methylsulfonyl derivatives) and involves a CBT

reagent that is 3-10 times cheaper than methylsulfonyl reagents, which increases possibilities for upscaling and broad use.

Next, we synthesized PAM hydrogels containing pendant CBT groups, denoted as PAM-CBT gels, by adapting a standard protocol for PAM hydrogels synthesis. Briefly, acrylamide (AM), bis-acrylamide (BIS) and CBT-AM were dissolved in water/DMF solution. After addition of the initiators, the polymerizing solution was placed on a hydrophobic glass slide and covered with an acrylated glass coverslip. Hydrogels were obtained after 30 min reaction, washed with deionized water, and wet-stored until use. By this means, thin PAM-CBT hydrogels were covalently attached to glass coverslips and proved stable for several months, making them a convenient platform for subsequent biofunctionalization, cell culture, and microscopy analysis (Figure 1B-C). Note that PAM-CBT hydrogels were obtained by a standard protocol and the overall reactivity of PAM formulation was not significantly altered by the incorporation of CBT-AM. This is in line with the preliminary studies shown above that indicated that the CBT moiety can withstand the free-radical initiation conditions used for PAM synthesis. Using a typical protocol for biomaterials preparation is advantageous, enabling this approach to be user-friendly for regular PAM users.

We confirmed the presence of CBT-AM in copolymerized hydrogels by spectroscopic means and studied the effect of its incorporation on hydrogel properties. The final concentration of CBT groups in PAM-CBT hydrogels could be controlled by adjusting the molar concentration of CBT-AM used during the synthesis. PAM-CBT hydrogels were synthesized with CBT-AM concentrations ranging 0 – 4 mol%, to yield materials that were colorless and transparent to the naked eye (Figure 1C). The presence of CBT groups in the hydrogels was corroborated by UV/Vis spectroscopy, where the spectra showed the distinctive absorption band of the CBT group at λ_{max} = 320 nm[18] (Figure 1D). Moreover, the intensity of the absorption band increased

linearly with the increase of CBT molar concentration in the hydrogels (Figure 1E), demonstrating the predictive control achieved on the loading of CBT groups into PAM hydrogels. Targeting CBT concentrations larger than 4 mol% was limited by CBT-AM solubility. Nevertheless, co-monomer concentrations of ≤ 4 mol% in PAM gels are deemed sufficient for adequate bioconjugation of ligands for cell culture.[11] Furthermore, we analyzed whether incorporation of increasing concentrations of CBT-AM impacted the properties of PAM-CBT hydrogels, in terms of swelling properties, stiffness, and microstructure (Figure 1 F-G). Increasing CBT-AM concentration from 0 to 4 mol% resulted in a slightly decreased hydrogel equilibrium swelling ratio (ESR varied from 95.2 to 84.6%), which was determined gravimetrically. Meanwhile, hydrogel thickness decreased from 79.3 to 47.5 μm as measured by confocal microscopy. In addition, the hydrogels Young's modulus increased from 1.9 to 6.0 kPa when increasing co-monomer concentration, as determined by nanoindentation (Figure 1H). These variations can be attributed to the hydrophobicity of the CBT moiety, which may lead to decreased water uptake at higher CBT-AM concentrations. This was in line with SEM analysis, that showed a decrease in the number of visible pores in the micrometer range and overall size of pores in the hydrogel microstructure, and more densely packed networks at increasing CBT-AM molar concentration (Figure S2). We noted, however, that PAM-CBT gels at 1 mol% concentration showed similar properties in terms of thickness and Young's modulus in relation to the 0 mol% hydrogel control (Figure 1 F-G). We anticipate that this is a relevant positive feature for cell culture experiments owing to the possibility of introducing a controlled CBT content while keeping other materials properties intact. Overall, our results demonstrate that CBT functional groups can be easily incorporated at controlled concentrations to PAM hydrogels.

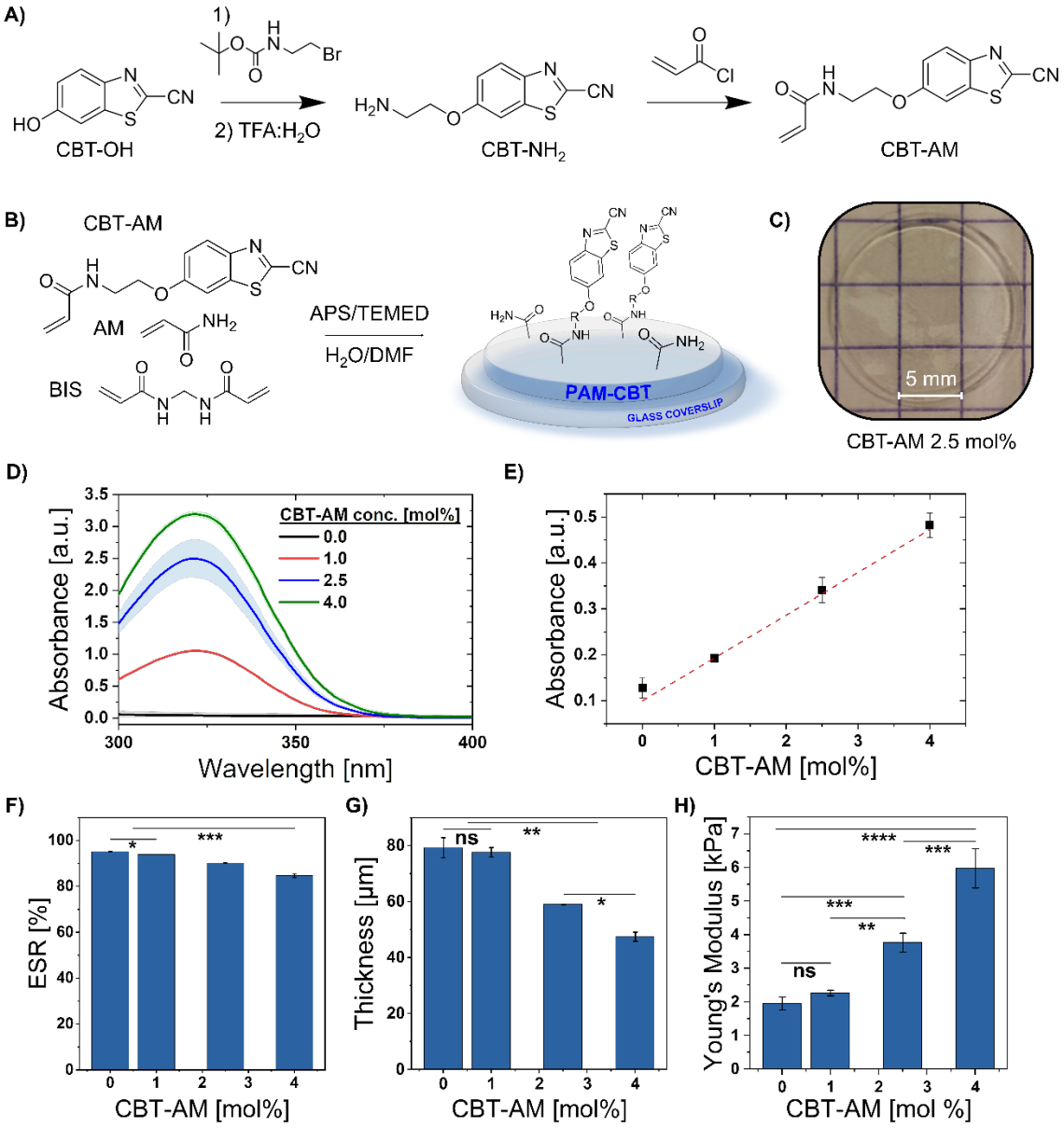

Figure 1. CBT-AM can be incorporated in PAM hydrogels at controlled loadings via standard protocols. (**A**) Synthesis pathway of CBT-AM co-monomer. (**B**) Schematics of the synthesis of PAM-CBT hydrogels and (**C**) photograph of a representative PAM-CBT hydrogel at 2.5 mol% CBT-AM concentration. (**D**) UV/Vis spectra of PAM-CBT hydrogels at increasing CBT-AM content and (**E**) absorbance value at λ= 360 nm (linear fit, adj. R-square = 0.98). (**F**) Equilibrium swelling ratio percentage, (**G**) thickness, and (**H**) Young's modulus of PAM-CBT hydrogels at increasing CBT-AM concentrations. Mean value and standard deviation (SD) shown, n = 3. Statistical analysis performed by one-way ANOVA followed by Tukey test; ns: not significant, * $p < 0.05$, ** $p < 0.01$, and *** $p < 0.001$.

2.2. Biofunctionalization of PAM-CBT hydrogels via luciferin click ligation

We studied the (bio)functionalization of PAM-CBT hydrogels at 2.5 mol% concentration of CBT-AM via luciferin click ligation using a fluorescent probe bearing an N-Cys functional group (Cys-dye) as a biomolecule surrogate (**Figure 2**A). Since our final aim was to apply this biofunctionalization strategy under mild conditions to preserve bioligand's activity, we performed the reaction in 20 mM HEPES buffer at pH 8, at room temperature, and with incubation times of up to 60 min. After incubation with the probe solution, hydrogels were washed with buffer to ensure removal of non-specifically absorbed dye, and measured using UV/Vis to prove the success of covalent immobilization of the dye. After modification, PAM-CBT hydrogels changed color (Figure 2B) and their UV/Vis spectra evidenced a new absorption band at λ_{max} = 504 nm, characteristic of the dye probe (Figure 2C). In comparison, a bare PAM hydrogel control that was identically treated did not show such absorption band. This indicates that a covalent immobilization occurs only in presence of CBT groups, which mediate a chemo-selective coupling to form luciferin-like adducts (Figure 2A).

To optimize experimental conditions for bioconjugation, biofunctionalization experiments were performed at constant Cys-dye concentration (1 mg mL^{-1}) and at increasing incubation times of 0-60 min. Under these conditions, the estimated CBT:Cys molar ratio was 10:1. After coupling, both hydrogel films and remnant incubation solution were measured using UV/Vis. The biofunctionalized PAM-CBT hydrogels evidenced that loading of the Cys-dye increased at increasing reaction times until reaching a plateau at 30 min (Figure 2D-E). This was in line with the complementary measurements performed on the remnant Cys-dye solution after incubation, which showed a decrease in the unbound Cys-dye at increasing reaction times (Figure S3B). We observed that after 5 min of incubation the concentration of unbound Cys-dye in the incubation solution already decreased to 17% of the starting value and that a further reduction

and a plateau value of <4% was reached at 30 min, thus supporting the observed quick coupling of Cys-dye to PAM under these experimental conditions.

Due to the high efficiency of luciferin click ligation, the amount of immobilized biomolecule can be finely controlled by modulating the probe concentration in the incubation solution. Regulating Cys-dye concentration from 0-1 mg mL^{-1} led to finely controlled biomolecule's loading in a reproducible manner (Figure 2F-G). This feature is particularly relevant considering that biological properties of PAM substrates could be significantly different according to their ligand density (e.g., density of cell-adhesive ligands).[10] Altogether, these results demonstrated that the covalent immobilization of a N-Cys-bearing biomolecule on PAM-CBT hydrogels is reproducibly achieved under mild conditions in short time and with controlled loading efficiency. In relation to previously reported methylsulfonyl co-monomers for thiol-mediated conjugation,[11] the present luciferin click ligation is expected to allow even higher chemo-selectivity, since in the latter an aminothiol group (~N-Cys moiety) is needed for coupling. Note that aminothiol groups are less frequent than thiols in biomolecules. This approach could be relevant for the site-specific immobilization of large bioligands via their N-terminal Cys moiety, thus avoiding undesired reactions that impair bioactive sites. Furthermore, the chemo-selective luciferin click ligation may be combined with other orthogonal coupling chemistries to enable specific control of the loading density of different ligands.

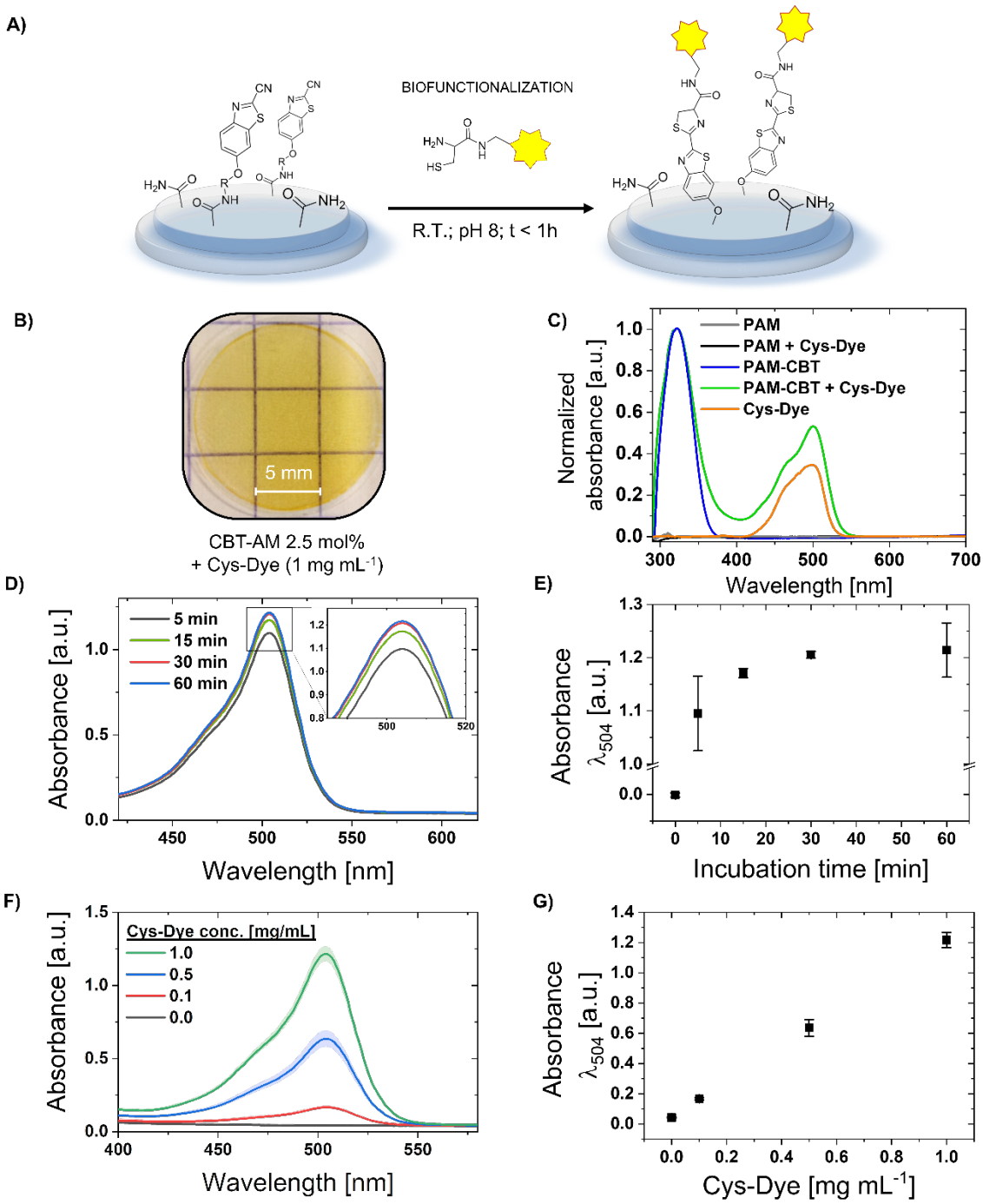

Figure 2. Biofunctionalization of PAM-CBT gels via luciferin click ligation is achieved at controlled biomolecule's loading and under mild aqueous conditions. (**A**) Schematic of the biofunctionalization of PAM-CBT hydrogels with Cys-dye probe. (**B**) Photograph of a PAM-CBT hydrogel at 2.5 mol% concentration after conjugation of Cys-dye. (**C**) Normalized UV/Vis absorbance of PAM and PAM-CBT hydrogels, before and after incubation with Cys-dye and compared to the Cys-dye solution. (**D-E**) Determination of the optimal incubation time for biofunctionalization at constant Cys-dye concentration (1 mg mL^{-1}) and (**F-G**) tuning of Cys-

dye loading upon incubation for 30 min at increasing biomolecule's concentration via UV/Vis analysis of the hydrogels. Conditions: PAM-CBT gel at 2.5 mol% concentration. Mean value and standard deviation (SD) shown, n = 3.

2.3. Comparison of luciferin click ligation to SS-mediated strategy for ligand loading

We compared the new biofunctionalization strategy based on luciferin click ligation onto PAM-CBT hydrogels with the most commonly applied strategy for biofunctionalization of PAM gels, which is mediated by SS photoactivation. Conditions for SS treatment and photo-activation of PAM gels were adapted from reported protocols to bind amine-bearing biomolecules.[20] Briefly, after two consecutive rounds of incubation of PAM with SS and illumination, the activated PAM-SS gels were incubated overnight with Cys-dye probe solution (1 mg mL^{-1}) and characterized by UV/Vis. In comparison, our approach based on luciferin chemistry enabled approximately 55-fold higher immobilization of Cys-dye than SS-based treatment of PAM hydrogels **(Figure 3A-B)** and within a much shorter time frame (30 min vs. overnight, respectively). This large difference highlights the relatively poor efficiency of SS-based immobilization, which is likely due to low incorporation of the SS-primer in PAM gels[10] or to side reactions that lead to inactivated photoproducts. Conversely, our PAM-CBT hydrogels presented a high degree of bioconjugation due to the efficiency of luciferin click ligation under mild conditions.

Furthermore, surface characterization of biofunctionalized hydrogels was performed by mapping the fluorescence intensity (at λ_{exc}= 488 nm) via confocal microscopy. PAM-CBT-dye hydrogels showed a homogeneous fluorescence intensity onto the surface, while PAM-SS-dye was characterized by inhomogeneities on the surface of the hydrogels (Figure 3C). This is in good agreement with previous reports that showed inhomogeneous immobilization of collagen I and Matrigel to PAM-SS hydrogels.[10, 21, 22] The authors speculated that these inhomogeneities

could be due to the proteins used, which could form bundles in solution before being conjugated to the hydrogel surface.[10] In our case, we used a small peptide as probe, which avoids the formation of aggregates of Cys-dye. Therefore, we hypothesize that the presence of inhomogeneities in SS-mediated conjugation may be related to the low solubility of SS and to the formation of precipitates during photoirradiation of the SS solution. In fact, during SS photoirradiation, we observed the precipitation of dark brown particles over the PAM surface, that could be due to the formation of insoluble reactive species (result not shown). This could lead to some regions of the PAM-SS surface containing a higher concentration of SS primer than others, ultimately leading to inhomogeneities during the immobilization of Cys-dye. Combined, our results show that luciferin click ligation outperforms the established SS-based strategy in terms of higher efficiency of ligand immobilization and increased homogeneity of the modified surface. We anticipate that the highly controlled, robust, and homogeneous biofunctionalization strategy achieved on PAM-CBT gels will be determinant for a reproducible biological activity of these materials.

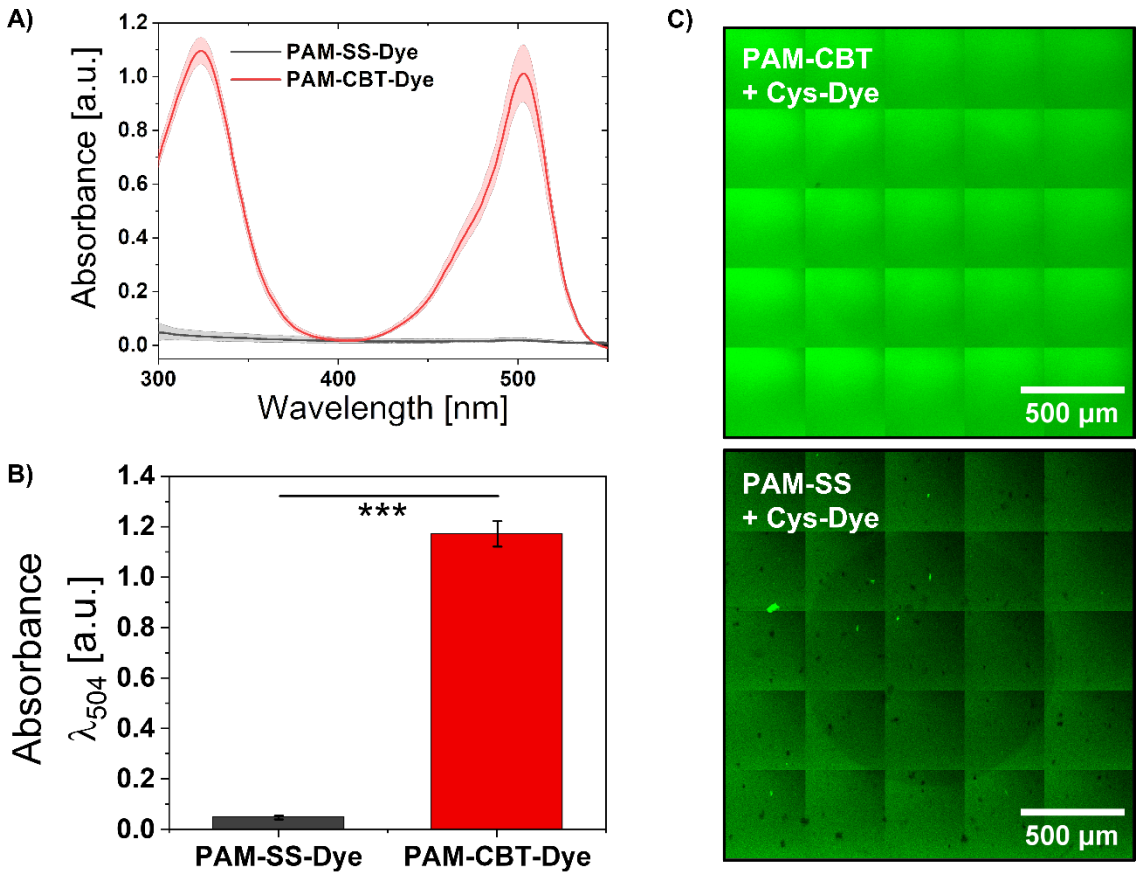

Figure 3. Luciferin click ligation strategy enables conjugation of higher payloads with increased homogeneity compared to sulfo-SANPAH (SS)-mediated strategy for biofunctionalization of PAM hydrogels. (**A**) UV/Vis spectra and (**B**) absorbance of immobilized dye at λ= 504 nm, of PAM-SS-dye and PAM-CBT-dye hydrogels after biofunctionalization. (**C**) Confocal fluorescence micrographs mapping the fluorescence intensity of the surface of PAM-CBT-dye and PAM-SS-dye hydrogels, at λ_{exc}= 488 nm. Scale bar: 500 µm. Statistical analysis performed via one-way ANOVA; n = 3; *** $p < 0.001$.

2.4. Cell culture studies

We then investigated the suitability of biofunctionalized PAM-CBT hydrogels as bioactive soft materials for 2D cell culture and compared it to the existing PAM-SS hydrogels. Besides the density of immobilized ligand, it is known that other materials properties, such as hydrogel stiffness, can affect cell behavior.[2, 23, 24] To decouple these effects, we kept the hydrogel

mechanics constant when comparing substrates functionalized by diverse chemical strategies. Thus, PAM-CBT gels with 1 mol% CBT concentration were selected and compared to PAM gels, since both substrates had comparable thickness and stiffness (Figure 1F-H). Following the above specified protocols, PAM-CBT and PAM-SS materials were biofunctionalized with RGD cell-adhesive peptide solution at the same concentration (1 mg mL^{-1}). The obtained PAM-CBT-RGD and PAM-SS-RGD hydrogels were then seeded with human mesenchymal stromal cells (hMSCs) to study cell adhesion, viability, and metabolic activity as a function of the hydrogel biofunctionalization strategy, over a cell culture period of 7 days. hMSCs (non-haematopoietic, multipotent cells) were chosen as a model cell type due to their capacity to differentiate into mesodermal (e.g., osteocytes, adipocytes and chondrocytes), ectodermal (neurocytes) and endodermal lineages (hepatocytes). hMSCs are generally accepted as suitable cell source for tissue engineering approaches and cell-based therapies, thus, with high potential for clinical translation.

Brightfield microscopy analysis was performed to investigate the cell adhesion process at relatively short culture times (i.e., from 30 min to 6 h). We observed that PAM-CBT-RGD hydrogels promoted remarkably faster cell adhesion than PAM-SS-RGD substrates. At 30 min post-seeding, hMSCs promptly begun to attach to PAM-CBT-RGD substrates, displaying increased cellular spreading. This was in stark contrast with PAM-SS-RGD substrates, in which even after 6 h, a large percentage of hMSCs still displayed very limited to no adhesion **(Figure 4A)**. Quantification of the percentage of cell adhesion at 1 h post-seeding was assessed by determining the total DNA collected from the cells that remained detached (procedure is schematized in Figure 4B). The results revealed that ~70% of cells adhered onto PAM-CBT-RGD; in contrast, only ~20% of hMSCs were adhered to PAM-SS-RGD (Figure 4C). This can be attributed to a higher ligand density attained on PAM-CBT gels, as inferred from above results with the fluorescent probe (Figure 2B), due to a more efficient coupling. It is also

possible that the chemo-selective luciferin click ligation led to preserved bioactivity of the ligand upon immobilization, contributing to a higher density of bioactive immobilized ligand. In contrast, the photoactivated SS-mediated strategy does not offer this control over site coupling, which could impair ligand's bioactivity, as suggested in prior work.[11]

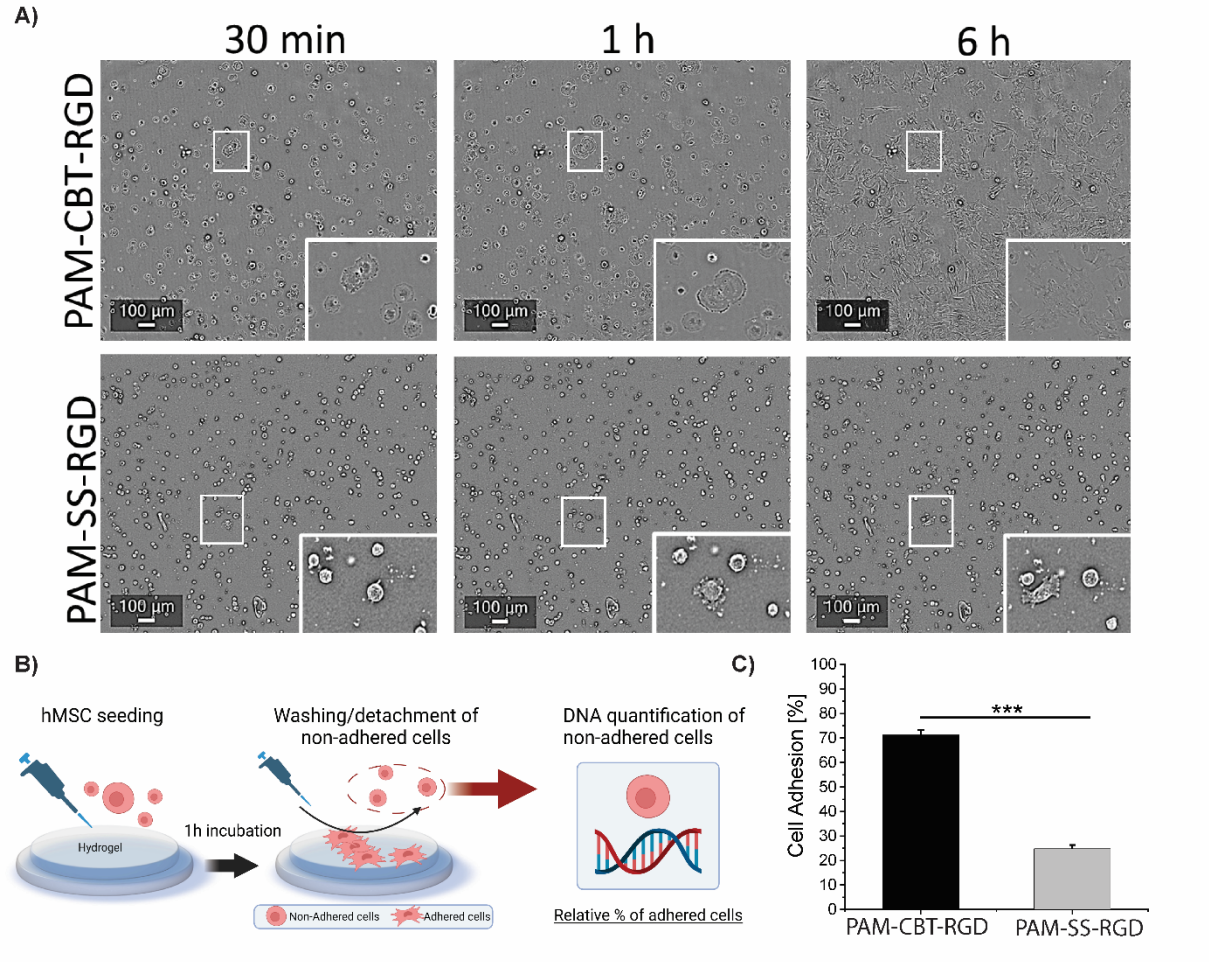

Figure 4. Controlled hydrogel biofunctionalization achieved via luciferin click ligation induces superior cell adhesion compared to SS-ligation. (**A**) Brightfield micrographs of hMSCs on top of PAM-CBT-RGD or PAM-SS-RGD at 30 min, 1 h and 6 h post-seeding. Scale bar: 500 µm. (**B**) Schematic representation of the stepwise approach for cell adhesion determination. (**C**) Quantification of the percentage of adhered cells 1 h after seeding, based on the quantification of total DNA collected from the non-adhered cell fraction at the cell suspension supernatant. Mean±SD shown, statistical analysis performed by one-way ANOVA, Tukey's post-hoc test, ***p< 0.001. Data shown is representative of 6 biological samples (n = 6) with two technical

duplicates. Conditions: 1 mol% PAM-CBT gel and PAM-SS gel, functionalized with 1 mg mL^{-1} RGD peptide solution. Initial cell density 2500 cells cm^{-2}.

We assessed if the increased cell adhesion on PAM-CBT-RGD at short culture times also correlated with increased metabolic activity and higher cell viability at longer culture timepoints, which would further corroborate cytocompatibility and high proliferative potential. hMSCs seeded on both PAM-CBT-RGD and PAM-SS-RGD hydrogels presented high levels of cytocompatibility, as virtually no dead cells were observed at days 1 and 7 post-seeding (**Figure 5**A). Interestingly, cell morphology correlated with the trend of the cell adhesion studies, as the hMSCs cultured on PAM-CBT-RGD displayed more elongated morphology and higher spreading throughout the hydrogel surface. It is worth mentioning that a more homogeneous cell attachment was observed on PEG-CBT-RGD hydrogels, and preliminary experiments showed that cells coverage was entirely uniform on the surface of this material after 7 days of culture (Figure S5A). Conversely, cells cultured on PEG-SS-RGD hydrogels evidenced noticeable aggregation and clustering (Figure 5A and Figure S5B), suggesting that cells likely sensed an underlying substrate with inhomogeneous and/or unactive biofunctionalization. This is in agreement with our results that demonstrated inhomogeneous surface modification of these substrates (Figure 3C). Therefore, hMSCs on PAM-SS-RGD hydrogels showed lower efficiency in recognizing the cell-adhesive ligand and instead preferred cell-cell contact, growing mostly in cell-based multilayered assemblies, thus avoiding contact with the material.

Moreover, hMSCs seeded on PAM-CBT-RGD displayed significantly higher cell metabolic activity at days 1, 3, and 7 than on PAM-SS-RGD (Figure 5B), indicating an overall higher proliferative potential of CBT-based hydrogels. This variation in cell proliferation across the different materials was confirmed by quantifying the amount of DNA, which was consistently higher for PAM-CBT-RGD substrates at the same timepoints (Figure 5C)**.** Altogether, the cell

studies confirm that PAM-CBT-RGD is a cytocompatible hydrogel that promotes fast hMSCs adhesion, which, in turn, correlated with significant stimulation of cell proliferation. In opposition, cells seem to have avoided the attachment onto PAM-SS-RGD hydrogels. This substrate, although being cytocompatible, promoted limited cell spreading even at longer timepoints, which greatly impacted cell proliferation. Our approach can be extended to biofunctionalize PAM gels with other N-Cys ligands and be useful for other cell types. For example, fibroblasts seeded on PAM-CBT-RGD hydrogels also showed high attachment capacity and spreading after 1 day (Figure S6B-C), while the control PAM-CBT, without RGD, displayed no cell attachment (Figure S6A).

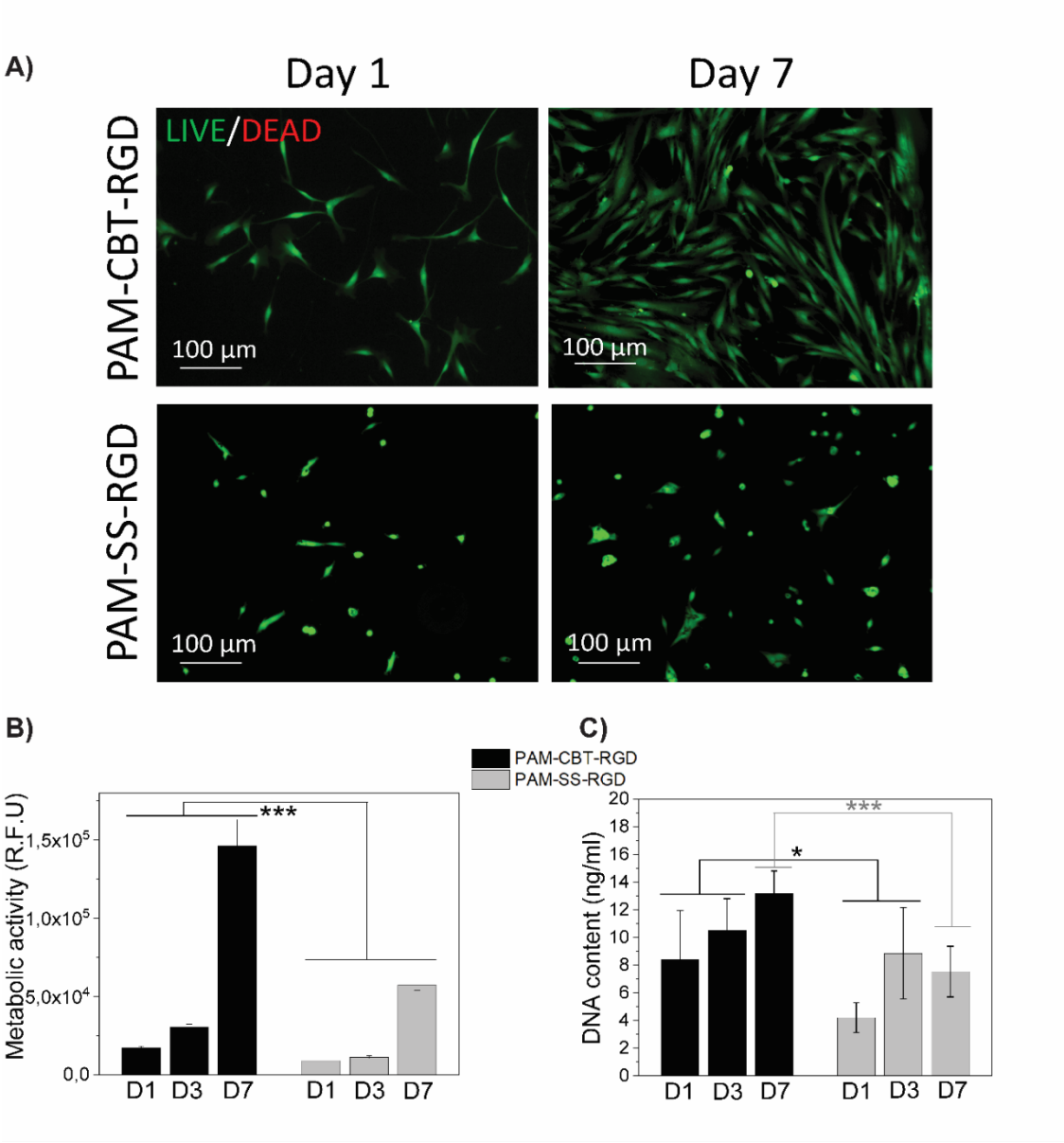

Figure 5. PAM-CBT-RGD hydrogels are cytocompatible and promote higher cell spreading and proliferation than PAM-SS-RGD substrates. (**A**) Live/Dead (Live – Green/CalceinAM; Dead – Red/Ethidium homodimer-1) fluorescence micrographs of hMSCs cultured on PAM-CBT-RGD vs PAM-SS-RGD hydrogels, at 1 and 7 days post-seeding. Scale bar: 100 µm. (**B**) Quantification of metabolic activity and (**C**) amount of total DNA recovered from the same experiments after 1, 3, and 7 days of seeding. Mean ± SD shown (one-way ANOVA, Tukey's post-hoc test ***$p < 0.001$, * $p < 0.05$). Data shown is representative of 6 biological samples each one measured in duplicate. Conditions: 1 mol% PAM-CBT gel and PAM gel, functionalized with 1 mg mL^{-1} RGD peptide solution. Initial cell density 2500 cells cm^{-2}.

Overall, the superior performance of PAM-CBT-RGD over PAM-SS-RGD hydrogels as biofunctionalized soft substrates that promote efficient cell attachment, spreading and proliferation might be attributed to a more effective and homogeneous immobilization of the cell-adhesive RGD peptide using luciferin click ligation. Furthermore, the characteristic chemo-selectivity of luciferin-based click ligation might preserve the functionality of the immobilized ligands, while SS-mediated reaction has been reported to partially impair RGD functionality, therefore weakening cell adhesion.[11]

3. Conclusions

CBT-AM incorporation into PAM hydrogels enabled luciferin click ligation as a highly efficient and robust bioconjugation strategy. PAM-CBT hydrogels were synthesized by regular protocols and biofunctionalized within minutes under mild conditions. PAM-CBT synthesis and ligand coupling were performed by a protocol that was simpler than the most commonly used PAM biofunctionalization strategy (e.g., SS chemistry). Furthermore, PAM-CBT outperformed SS strategy in biofunctionalization efficiency and homogeneity, which led to remarkable differences in the biofunctionality of the substrates. These results highlight the importance of having efficient, reliable, and reproducible biofunctionalization strategies to generate more controlled ECM-mimicking models in PAM hydrogels. Hence, the presented strategy is anticipated to promote more conclusive studies regarding cell-ligands interaction by enabling a better control of ligand density loading.

4. Materials and Methods

4.1 Reagents and instrumentation

Reagents and solvents were obtained from commercial sources and used as received, unless otherwise stated. The peptides cyclo(Arg-Gly-Asp-D-Phe-Lys(Cys)) c[RGDfK(C)] and Cys-

PEG_3-Lys(Fluorescein)-NH_2 (Cys-dye) were purchased from Genecust and cyclo(Arg-Gly-Asp-D-Phe-Lys) (c[RGDfK]) from Bioshynt. The co-monomer N-(2-((2-cyanobenzo[d]thiazol-6-yl)oxy)ethyl)acrylamide (CBT-AM) was synthesized as detailed in the Supplementary Information. UV/Vis spectra were recorded with a Varioskan Lux plate reader. UV-light irradiation was carried out with a UV-KUB 2 (365 nm, 50 mW cm^{-2}).

4.2 Hydrogels preparation, biofunctionalization and characterization

Acrylation of glass coverslips:

An adapted protocol was followed.[25] Round glass coverslips (15 mm diameter) were acryl-silanized by overnight incubation with 1% v/v solution of 3-acryloxypropyl-trimethoxysilane (APM, dissolved in ethanol (95% v/v) and water (4% v/v)). To stabilize the interface, the coverslips were washed with ethanol and water and then exposed to at 80 ˚C in vacuum for 1 h.

Hydrogels synthesis:

PAM and PAM-CBT hydrogels were synthesized using an adapted protocol.[25] The total concentration of vinyl groups was kept constant at 1.77 M (100 mol%) by adjusting the relative concentration of acrylamide (AM) and CBT-AM while *N,N′*-methylenebisacrylamide (BIS) concentration was constant (4.28 10-2 M). Briefly, AM (91.2 – 95.2 mol%) was dissolved in deionized water and added to a solution of CBT-AM (0 – 4 mol%) and BIS (2.4 mol%) in DMF to form a 1:1 volume water:DMF mixture. The mixture was deoxygenated by N_2 bubbling and the initiator ammonium persulfate (APS) (10% solution, 4/100 of total volume) and *N,N,N′,N′*-tetramethylethylenediamine catalyst (TEMED) (4/100 of total volume) were added. A 10 µL droplet of the polymerizing solution were placed on hydrophobic-coated glass slides and covered with the prepared acrylated glass coverslips. After 30 min of polymerization reaction, the coverslips were immersed in deionized water for 1 h before gently detaching the hydrogels from the hydrophobic-coated slides. The hydrogels, covalently attached to the acrylated coverslips, were kept in deionized water until further use.

Biofunctionalization of PAM-CBT hydrogels via luciferin click ligation:

PAM-CBT hydrogels were modified with the N-Cys-biomolecules, namely the cell adhesive peptide c[RGDfK(C)] or the fluorescent dye Cys-PEG_3-Lys(Fluorescein)-NH_2 (Cys-dye). The peptides were dissolved in HEPES buffer (20 mM, pH 8.0) containing TCEP (0.5 eq. with respect to Cys-peptide moles). A 40-µL droplet of ligand solution was placed over a parafilm surface and a hydrogel disc was placed on top, with the hydrogel thin layer facing down. The coupling reaction occurred at room temperature during 30 min (unless otherwise stated) followed by washing with HEPES buffer and PBS to ensure removal of non-specifically absorbed ligand.

Biofunctionalization of PAM hydrogels mediated via sulfo-SANPAH (SS) treatment:

Bare PAM gels were treated with sulfo-SANPAH (SS) before immobilization of amine-bearing ligands, following previously published protocols.[20] PAM hydrogel was covered with 100 µL of SS solution (0.5 mg mL^{-1} in HEPES, 50 mM, pH 8.5) and immediately irradiated with UV-light (365 nm, 50 mW cm^{-2}) during 5 min. Hydrogels were rinsed with HEPES buffer (50 mM, pH 8.5) and the previous incubation and irradiation steps were repeated once again. After rinsing with HEPES (20 mM, pH 8.0), hydrogels were incubated with 40 µL of ligand solution (in HEPES 20 mM, pH 8.0) at room temperature overnight. Substrates were washed with HEPES buffer and PBS to ensure removal of non-specifically absorbed ligand.

UV/Vis characterization:

Hydrogel samples, before and after immobilization of the Cys-dye, were placed at the bottom of 24-well plates and measured. In parallel, the amount of immobilized ligand was estimated by an indirect procedure as follows. After incubation of the hydrogels with the Cys-dye solution for a desired time, an aliquot (10 µL) of the remnant incubation solution was taken and diluted 1:6 in HEPES buffer. The absorbance of the solution at λ = 496 nm was measured (n=3 for each

time point) and, via the Lambert-Beer law, contrasted with a calibration curve elaborated using solutions of known concentrations of the Cys-dye (0 - 0.1 mg mL-^{1}). Finally, the concentration of remnant dye in solution was inferred from a linear regression in the calibration curve (R^2 = 0.998).

Scanning electron microscopy (SEM):

Hydrogel films were dehydrated stepwise in ethanol and subsequently critically point dried (EM CPD300, Leica). Dried samples were sputtered with gold and investigated by SEM (JST-IT100, JEOL) operated at 5kV in scanning mode.

Confocal microscopy:

Hydrogel thickness was determined by imaging with a Zeiss LSM 880 confocal microscope using a Plan-Apochromat 20x/0.80 M27 air objective. Hydrogel samples (either PAM-CBT-dye or PAM-SS-dye) that contained the fluorescent probe Cys-dye were imaged (λ_{exc} = 488 nm) in the tile scan mode (1953x1953 μm) combined with Z-stack mode. Hydrogels thickness was measured by following the Z-axis intensity profile of the fluorescent signal of the fluorophore.

Mechanical characterization of hydrogels by nanoindentation:

The local Young's modulus of the hydrogel formulations was measured using an interferometry-based nanoindenter (Optics11 life), equipped with a probe with a cantilever stiffness of 0.26 N m^{-1} and a tip radius of 22.5 μm. Samples were indented to a depth of 1 μm and the Young's modulus was obtained applying a Hertzian fit to the load curve (assuming a Poisson ratio of 0.5). N=3 hydrogel samples were measured per condition and 10 measurements were performed on each sample. Data was expressed as mean ± SD.

Equilibrium swelling ratio of hydrogels:

Following the above procedure, PAM-CBT hydrogels with different CBT-AM content were prepared in 3-mL plastic syringes and cured for 30 min at room temperature. The resulting hydrogels were carefully demolded, cut into discs, and swelled in 1x PBS buffer, pH 7.4 at room temperature for 24 h. The mass of swollen hydrogels was measured (m_s) and then the hydrogels were freeze-dried to measure the mass of dry gels (m_d). The equilibrium swelling ratio (ESR) was calculated according to equation 1:

$$\text{ESR} = \frac{m_s - m_d}{m_d} \times 100 \text{ (equation 1)}$$

Experiments were performed in 4 replicates. Data was expressed as mean ± SD.

Statistical analysis:

Data were expressed as mean ± standard deviation (SD). For each condition, a minimum of 3 independent experiments were performed. In all cases, a value of $\alpha < 0.05$ was used for statistical significance. A one-way ANOVA with a Tukey test of the variance was used to determine the statistical significance between groups.

4.3 Cell culture

Cell culture protocols:

Human mesenchymal stromal cells (hMSCs) were isolated from fresh bone marrow, seeded in tissue culture flasks at a density of 500,000 cells cm^{-2} and cultured in hMSC proliferation media, comprised of 10% FBS, 100 U mL^{-1} penicillin and 100 µg mL^{-1} streptomycin, 1% GlutaMAX, 0.2 mM ascorbic acid and 1 ng mL^{-1} bFGF. Upon confluency, cells were detached using 0.25% (w/v) trypsin-EDTA at 37°C and subcultured for posterior experiments.

Cell seeding optimization for brightfield microscopy analysis was performed by seeding $2.5x10^3$, $5x10^3$ and $10x10^3$ cells cm^{-2} on top of each hydrogel substrate contained within a 24-well plate. A cell seeding density of $2.5x10^3$ cells cm^{-2} was defined as optimal to obtain single

cell resolution for visual attachment analysis at early timepoints. Post-seeding, cells were incubated at 37°C, 5% CO_2 and visualized using a CellCyte X in-incubator live cell imager (Cytena) programmed to microphotograph the sample every 30 minutes for a period of 24 h.

Cell adhesion quantification:

Cell adhesion was quantified by collection of the supernatant containing the non-adhered cell fraction at 1 h post-seeding and respective DNA quantification was performed using the Quantifluor Double-Stranded DNA (dsDNA) system kit (Promega), according to the manufacturer's instructions. Samples were prepared by seeding $7.5x10^3$ cells cm^{-2}, and the non-adhered cell fraction in the supernatant was collected at each time point and centrifuged for 5 min at 300 G. The cell pellet was then washed with lysis buffer (0.1 M KH_2PO_4, 0.1 M K_2HPO_4 and 0.1% Triton X-100) and the lysate was transferred to a new Eppendorf vial and frozen at -20°C until dsDNA quantification was performed. The percentage of cell adhesion was determined by comparing the amount of dsDNA on each hydrogel to an equivalent non-RGD functionalized hydrogel (control). Three biological samples comprised of two technical replicates were used for cell adhesion quantification.

Metabolic activity quantification:

Metabolic activity was determined by PrestoBlue Cell Viability Reagent (Thermofisher) at days 1, 3, and 7 timepoints after cell seeding (density $2.5x10^3$ cells cm^{-2}). PrestoBlue stock reagent was diluted 1:10 in hMSCs proliferation media, warmed at 37°C and added to each well (24-well plate). The plate was then protected from light using aluminum foil and incubated at 37°C 5% CO_2 for 2 h. After incubation, the supernatant was collected and transferred to a white lumiNunc plate 96-well plate. Fluorescence was immediately read on a Perkin Elmer LS50B plate reader (λ_{exc}= 545 nm, λ_{em}= 590 nm). Prestoblue with media and without cells was used as

fluorescence background control. Metabolic activity was determined by quantification of relative fluorescence units (RFUs).

Supporting Information

Supporting Information is available from the author.

Acknowledgements

The authors thank financial support from the Deutsche Forschungsgemeinschaft (DFG, project no. 422041745) awarded to JIP.

References

[1] Z. Chen, L. Kang, Z. Wang, F. Xu, G. Gu, F. Cui, Z. Guo, *RSC Adv.* **2014**, 4, 63807.
[2] R. J. Pelham, Y.-l. Wang, *Proceedings of the National Academy of Sciences* **1997**, 94, 13661.
[3] C. O. Heras-Bautista, N. Mikhael, J. Lam, V. Shinde, A. Katsen-Globa, S. Dieluweit, M. Molcanyi, V. Uvarov, P. Jutten, R. G. A. Sahito, F. Mederos-Henry, A. Piechot, K. Brockmeier, J. Hescheler, A. Sachinidis, K. Pfannkuche, *Acta Biomater* **2019**, 89, 180.
[4] A. M. Cozzolino, V. Noce, C. Battistelli, A. Marchetti, G. Grassi, C. Cicchini, M. Tripodi, L. Amicone, *Stem Cells Int* **2016**, 2016, 5481493.
[5] C. Bruyere, M. Versaevel, D. Mohammed, L. Alaimo, M. Luciano, E. Vercruysse, S. Gabriele, *Sci Rep* **2019**, 9, 15565.
[6] J. R. Tse, A. J. Engler, *Curr Protoc Cell Biol* **2010**, Chapter 10, Unit 10 16.
[7] L. Liu, Q. Liu, A. Singh, in *Proteins at Interfaces III State of the Art*, Vol. 1120, American Chemical Society **2012**, Ch. 30, p. 661.
[8] A. Wolfel, M. Jin, J. I. Paez, *Frontiers in Chemistry* **2022**, 10.
[9] Y. Aratyn-Schaus, P. W. Oakes, J. Stricker, S. P. Winter, M. L. Gardel, *J Vis Exp* **2010**, DOI: 10.3791/2173.
[10] S. Lee, A. E. Stanton, X. Tong, F. Yang, *Biomaterials* **2019**, 202, 26.
[11] A. Farrukh, J. I. Paez, M. Salierno, A. del Campo, *Angewandte Chemie International Edition* **2016**, 55, 2092.
[12] A. Farrukh, J. I. Paez, M. Salierno, W. Fan, B. Berninger, A. del Campo, *Biomacromolecules* **2017**, 18, 906.
[13] E. H. White, F. McCapra, G. F. Field, *Journal of the American Chemical Society* **1963**, 85, 337.
[14] H. Ren, F. Xiao, K. Zhan, Y.-P. Kim, H. Xie, Z. Xia, J. Rao, *Angewandte Chemie International Edition* **2009**, 48, 9658.
[15] Z. Chen, M. Chen, Y. Cheng, T. Kowada, J. Xie, X. Zheng, J. Rao, *Angewandte Chemie International Edition* **2020**, 59, 3272.
[16] H. Karatas, T. Maric, P. L. D'Alessandro, A. Yevtodiyenko, T. Vorherr, G. J. Hollingworth, E. A. Goun, *ACS Chemical Biology* **2019**, 14, 2197.
[17] A. Godinat, H. M. Park, S. C. Miller, K. Cheng, D. Hanahan, L. E. Sanman, M. Bogyo, A. Yu, G. F. Nikitin, A. Stahl, E. A. Dubikovskaya, *ACS Chemical Biology* **2013**, 8, 987.
[18] M. Jin, G. Koçer, J. I. Paez, *ACS Applied Materials & Interfaces* **2022**, 14, 5017.

[19] M. A. Gauthier, M. I. Gibson, H.-A. Klok, *Angewandte Chemie International Edition* **2009**, 48, 48.
[20] F. Mustapha, K. Sengupta, P. H. Puech, *STAR Protoc* **2022**, 3, 101133.
[21] J. H. Wen, L. G. Vincent, A. Fuhrmann, Y. S. Choi, K. C. Hribar, H. Taylor-Weiner, S. Chen, A. J. Engler, *Nat Mater* **2014**, 13, 979.
[22] B. Trappmann, J. E. Gautrot, J. T. Connelly, D. G. Strange, Y. Li, M. L. Oyen, M. A. Cohen Stuart, H. Boehm, B. Li, V. Vogel, J. P. Spatz, F. M. Watt, W. T. Huck, *Nat Mater* **2012**, 11, 642.
[23] H. Long, B. E. Vos, T. Betz, B. M. Baker, B. Trappmann, *Adv Sci (Weinh)* **2022**, 9, e2105325.
[24] J. Xie, M. Bao, X. Hu, W. J. H. Koopman, W. T. S. Huck, *Biomaterials* **2021**, 267, 120494.
[25] J. I. Paez, A. Farrukh, O. Ustahüseyin, A. del Campo, in *Biomaterials for Tissue Engineering: Methods and Protocols*, DOI: 10.1007/978-1-4939-7741-3_8 (Ed: K. Chawla), Springer New York, New York, NY **2018**, p. 101.